

Title	Electrodeposited thin-film micro-thermoelectric coolers with extreme heat flux handling and microsecond time response
Authors	Corbett, Simon;Gautam, D.;Lal, Swatchith;Yu, Kenny;Balla, Naveen;Cunningham, Graeme;Razeeb, Kafil M.;Enright, Ryan;McCloskey, David
Publication date	2021-01-04
Original Citation	Corbett, S., Gautam, D., Lal, S., Yu, K., Balla, N., Cunningham, G., Razeeb, K. M., Enright, R. and McCloskey, D. (2021) 'Electrodeposited thin-film micro-thermoelectric coolers with extreme heat flux handling and microsecond time response', ACS Applied Materials and Interfaces, 13(1), pp. 1773-1782. doi: 10.1021/acsami.0c16614
Type of publication	Article (peer-reviewed)
Link to publisher's version	10.1021/acsami.0c16614
Rights	© 2021, American Chemical Society. This document is the Accepted Manuscript version of a Published Work that appeared in final form in ACS Applied Materials and Interfaces, after technical editing by the publisher. To access the final edited and published work see: https://doi.org/10.1021/acsami.0c16614
Download date	2024-04-24 04:56:25
Item downloaded from	https://hdl.handle.net/10468/11071

Supporting Information: Electrodeposited thin film micro-thermoelectric coolers with extreme heat flux handling and microsecond time response

Simon Corbett¹, D. Gautam⁴, Swatchith Lal⁴, Kenny Yu^{1,3}, Naveen Balla², Graeme Cunningham^{1,2}, Kafil M. Razeeb⁴, Ryan Enright³, David McCloskey^{1,2}

¹ School of Physics, Trinity College Dublin 2, D02PN40, Ireland.

² AMBER Centre, CRANN Institute, Trinity College Dublin, Dublin 2, D02PN40, Ireland

³ Thermal Management Research Group, Efficient Energy Transfer (η ET) Department, Nokia Bell Labs, D15 Y6NT, Ireland.

⁴ Tyndall National Institute, University College Cork, Dyke Parade, Lee Maltings, Cork T12 R5CP, Ireland.

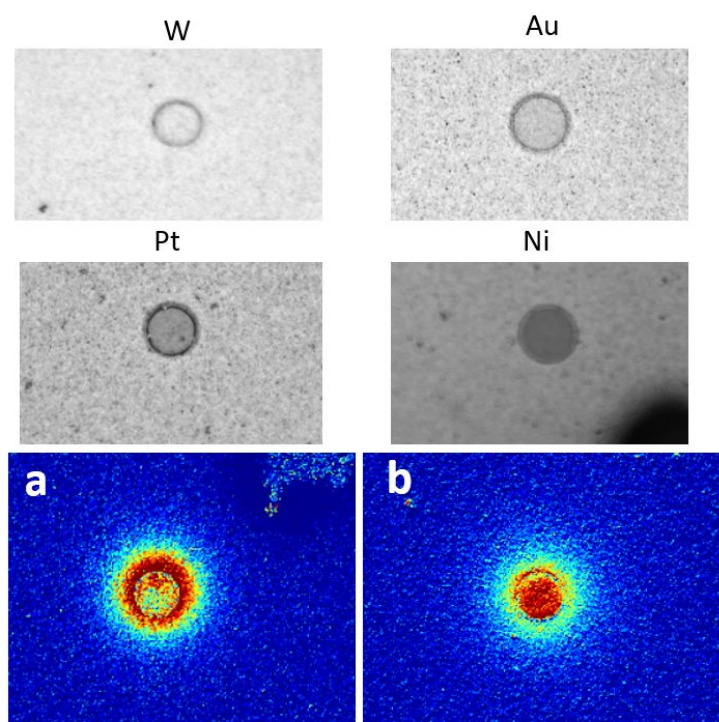
Corresponding Authors

* Email: corbetsi@tcd.ie, dmcclosk@tcd.ie, kafil.mahmood@tyndall.ie

Supplementary Tables

Table S1. Parameters used for Finite Element method simulation.

Material	Thermal Conductivity $\text{WK}^{-1}\text{m}^{-1}$	Seebeck Coefficient μVK^{-1}	Electrical Conductivity Sm^{-1}
Au [1, 2]	200	6.5	45.6×10^6
W [2, 3]	20	7.5	20×10^6
SiN [4]	2	-	1.2×10^{-18}
Bi_2Te_3	As measured	As measured	As measured
SiO_2 [5]	1.4	-	1×10^{-18}
Si [5]	130	-	5×10^{-4}



Supplemental Figures

*Figure S1 Optical images showing various metal contacts and their diffusion into the TE layer.
Example of temperature maps from **a)** a bad metal contact and **b)** a W contact.*

Initially several samples as in Fig.1a were made with a different metal replacing the W top contact layer. There was a noticeable degradation of the top contact with each as can be seen in Fig S.1 in the contrast between the circular pads. This is evidence of diffusion of the top layer metal layers into the Bi_2Te_3 beneath. Most of the pads could not be electrically contacted and those that could be, produced non ideal temperature maps as in Fig. S1.a. This ring of elevated temperature around the pad is evidence of current crowding and suggests that the top circular contact is physically receding beneath the SiN layer. Past a critical point there will be no circuit and the device will no longer work. Fig.S1.b shows an ideal temperature map typically produced by the W samples.

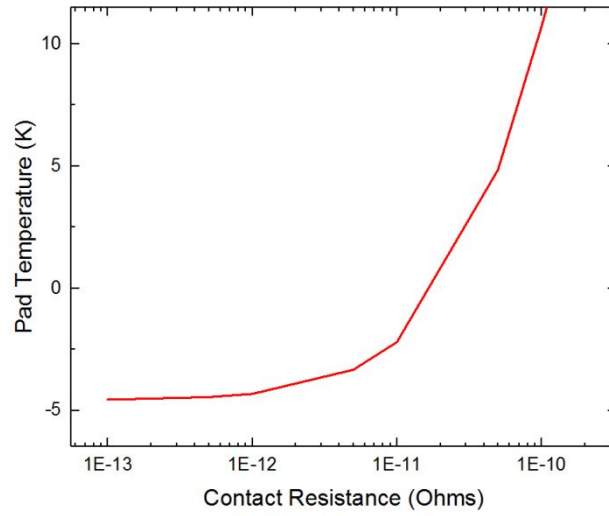


Figure S2. The effect of contact resistance on the top pad temperature.

FEM simulations were carried out with various contact resistances input at the top and bottom of the thermoelectric layer. Figure S2 shows the effect on the temperature rise for the top Au layer under a 200mA cooling current. The simulated results show that no net temperature differential would be allowed with contact resistance over $10^{-11} \Omega \cdot \text{m}^{-2}$. The increased contact resistance increases the joule heating at the interface thus lowering the possible achievable temperature difference.

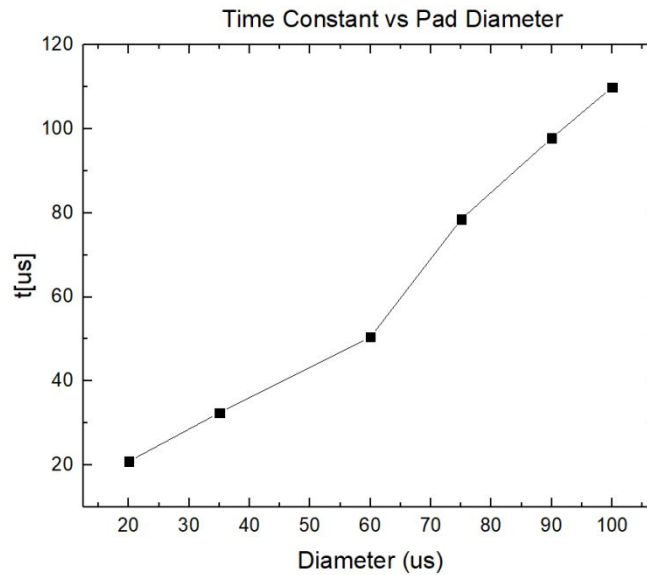


Figure S3. Time constant of cooling for various pad diameters.

FEM simulations showed that the cooling response times varied linearly on the diameter of the contact pad. As the contact pad diameters increased in size, the active region of the TE increased proportionally.

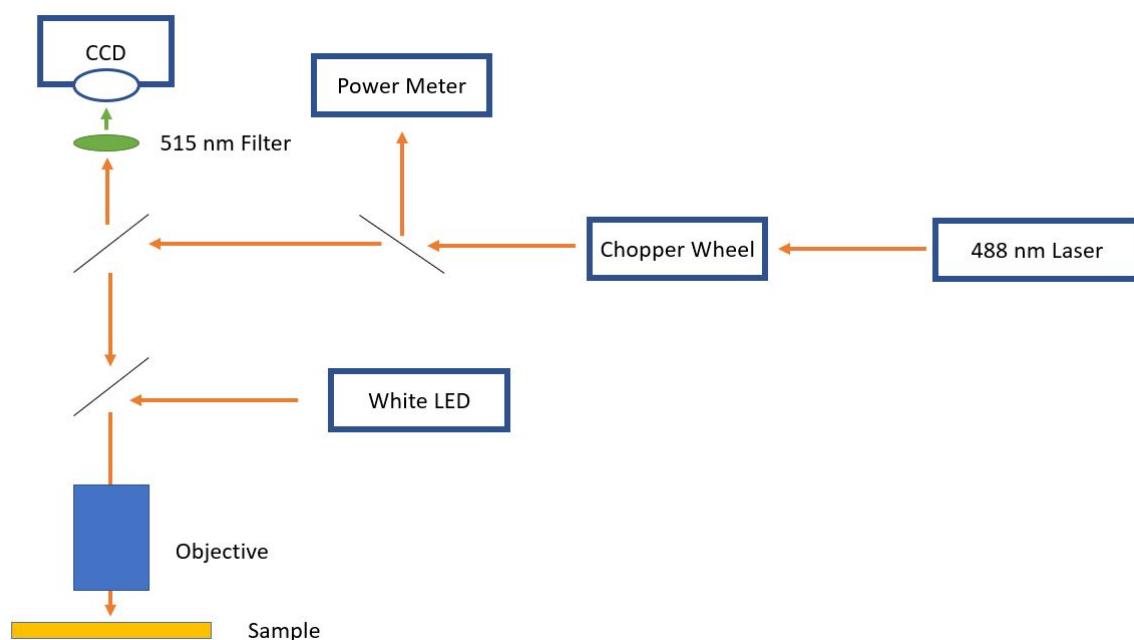


Figure S4 Optical pathway for the laser induced heating and CCD-TR setup.

An adaptation of the standard CCD-TR setup allows a laser to be used to induce a temperature rise on the top surface. The CCD camera is triggered to expose twice over the period of the chopped laser power such that two images are captured; one when the device is “hot” and the other “cold”. The difference in intensity between the two images is the change in reflectivity due to thermoreflectance of the Au top surface from which the temperature can be extracted. The 515 nm filter is chosen for the peak sensitivity in golds thermoreflectance spectrum.

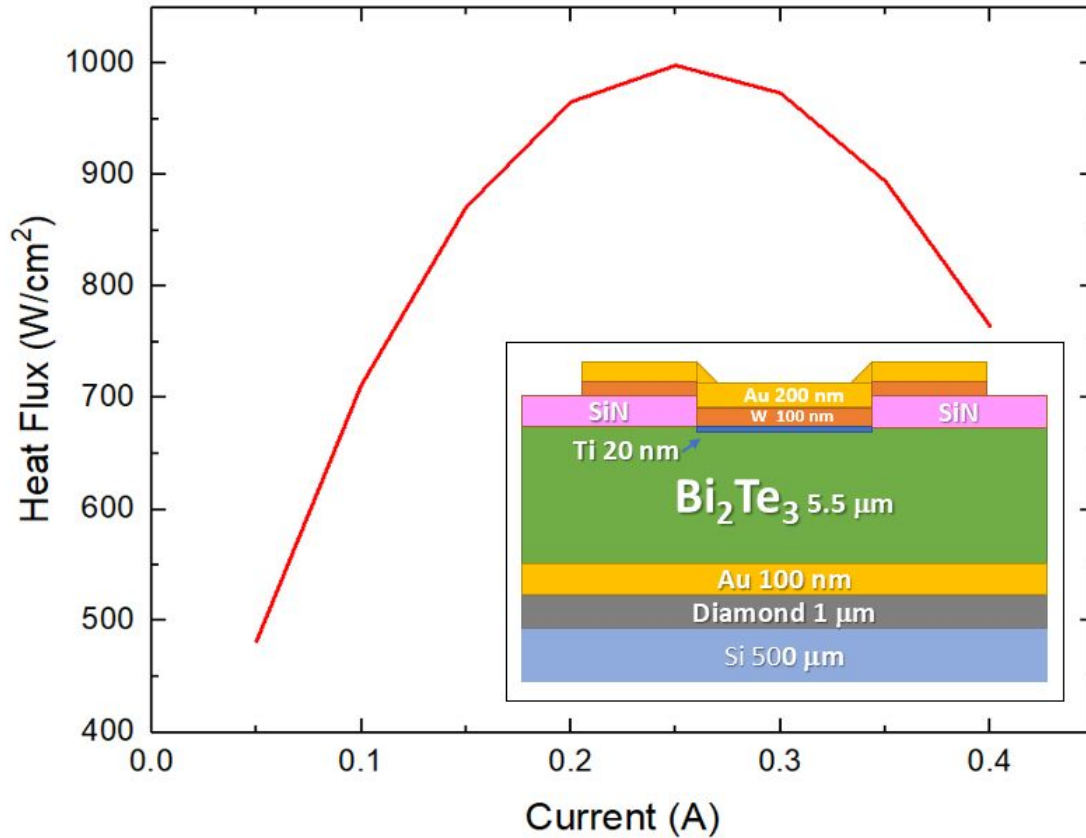


Figure S5 Cooling heat flux for various cooling currents with more ideal diamond substrate. Inset shows the diamond substitution layer instead of the silicon oxide layer.

The cooling heat flux of this device is limited due to the non-ideal design of this cooler with a low thermal conductivity layer of SiO₂. This essentially chokes the ability of the TE device to pump the heat downwards into the substrate at the hot side. If this layer was instead replaced by CVD grown diamond substrate with a thermal conductivity^{S1} of 2200 Wm⁻¹K⁻¹ max theoretical heat flux of 1000 Wcm⁻² can be achieved.

S1 - <http://www.iiviinfrared.com/Optical-Materials/thermal-grade-CVD.html>

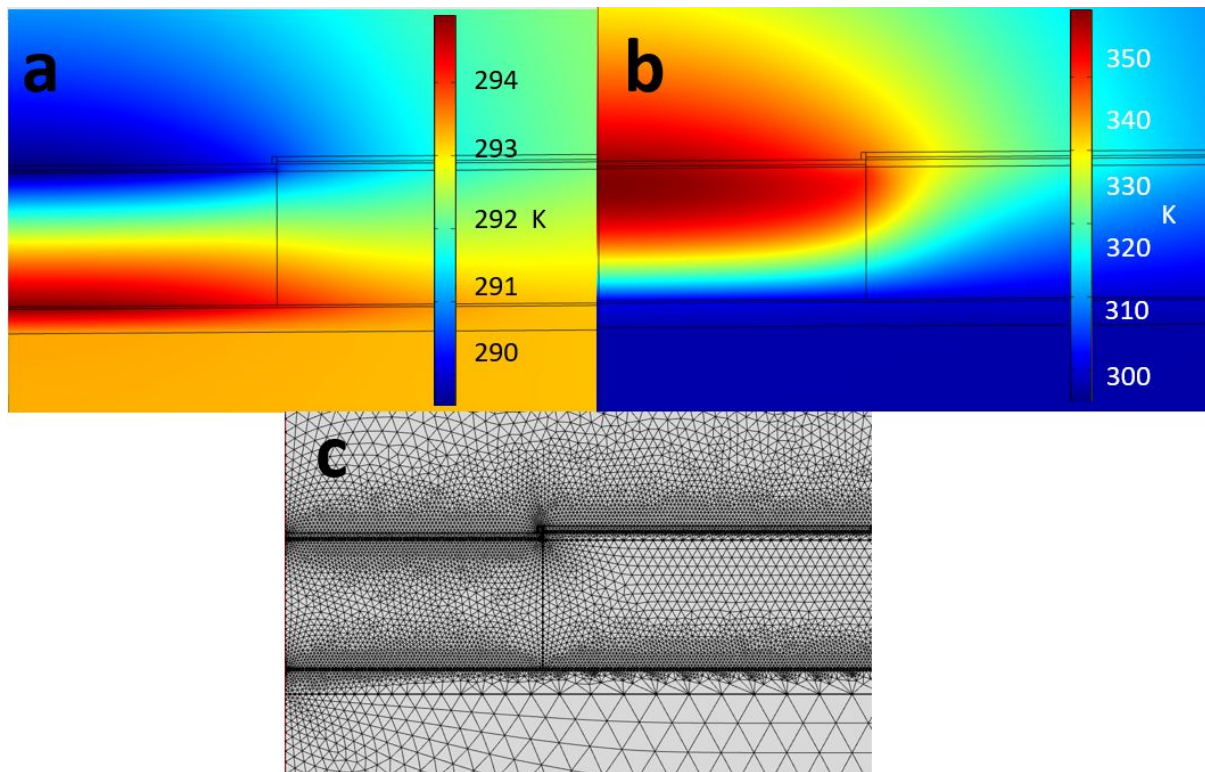


Figure S6 a) Example of cross section showing temperature gradient across device in cooling mode b) Example of cross section showing temperature gradient across device in cooling mode c) The same cross section showing the meshing size used in the COMSOL model.

A clear different is seen between the magnitude of the thermal gradients in Figure S6.a, S6.b which show a modelled cross-section of the device as it is cooling the top surface and heating it respectively. This simulation does not take into account the Thomson effect or changes in thermal parameters with temperature. If the Thomson coefficient is taken to be negative then this would have the effect of reducing the magnitude of the top temperature of the TE device. A rough calculation of the relative magnitude of the Thomson effect to the total heat generated by the TE material is 10% for a temperature difference of 50°C across the device induced by a 300mA current.

1. Langer, G., J. Hartmann, and M. Reichling, *Thermal conductivity of thin metallic films measured by photothermal profile analysis*. Review of Scientific Instruments, 1997. **68**(3): p. 1510-1513.
2. Lasance, C.J.M. *Seebeck coefficients for various metals*. 2006. DOI: <https://www.electronics-cooling.com/2006/11/the-seebeck-coefficient/>.
3. Martan, J., et al., *Thermal Characterization of Tungsten Thin Films by Pulsed Photothermal Radiometry*. Nanoscale and Microscale Thermophysical Engineering, 2006. **10**: p. 333-344.
4. J.~Kuntner, et al., *Determining the thin-film thermal conductivity of low temperature PECVD silicon nitride*. 2006.
5. *COMSOL Material Library*, COMSOL, Editor. 2020.